Three-chain B6n+14 cages as possible precursors for the syntheses of boron fullerenes

Haigang Lu and Si-Dian Li

Citation: The Journal of Chemical Physics **139**, 224307 (2013); doi: 10.1063/1.4839575
View online: http://dx.doi.org/10.1063/1.4839575
View Table of Contents: http://scitation.aip.org/content/aip/journal/jcp/139/22?ver=pdfcov
Published by the AIP Publishing

Three-chain B_{6n+14} cages as possible precursors for the syntheses of boron fullerenes

Haigang Lu[a] and Si-Dian Li
Key Laboratory of Chemical Biology and Molecular Engineering of the Education Ministry, Institute of Molecular Science, Shanxi University, Taiyuan, Shanxi 030006, People's Republic of China

(Received 4 July 2013; accepted 20 November 2013; published online 11 December 2013)

Using the first principle methods, we proposed a series of three-chain boron cages B_{6n+14} (n = 1–12) which are mainly built by fusing three boron semi-double-rings. Their simple geometric structures (approximate D_3 or C_3 symmetry) facilitate their bottom-up syntheses from the hexagonal B_7 and the double-chain boron clusters, such as B_2, B_4, B_6, B_8H_2, $B_{10}H_2$, $B_{12}H_2$, and the double ring B_{20}. The spherical shapes of these three-chain boron cages show that they could be taken as the possible precursors to further synthesize the boron fullerenes, such as B_{80}. Therefore, these three-chain boron cages provide a possible synthesis pathway of the boron fullerenes from the experimentally synthesized small planar boron clusters. © *2013 AIP Publishing LLC*. [http://dx.doi.org/10.1063/1.4839575]

Since the striking developments of carbon fullerenes, many boron fullerenes have been proposed theoretically in search of new materials. The famous B_{80} fullerene proposed by Szwacki *et al.* has structural resemblance with the C_{60} fullerene, and has 12 pentagons and 20 hexagons, with the 20 additional boron atoms capping the hexagonal rings.[1] Subsequently it was shown that other less symmetric bulk-like precursors, dubbed core-shell structures, are energetically preferred.[2–5] However, De *et al.* had shown that the energy landscape of boron clusters is glasslike and larger boron clusters have many structures which are lower in energy than the cages so that the boron fullerenes, such as B_{80}, are difficult to be synthesized and/or characterized in experiment.[6] Cage-doping is one of the possible synthesis pathways of the boron fullerenes.[7]

In recent years, many small boron clusters and boron-rich clusters have been found as individual species in the gas phase by joint experimental and theoretical investigations.[8–19] The B_n (n < 20) clusters possess (quasi-)planar structures, in which the hexagonal boron cluster B_7 is one of the basic units in the Aufbau principle for boron clusters.[20,21] The $B_nH_2^{-/0}$ (n = 7–12) and $B_nH_2^{2-}$ (n = 6–22) clusters have a double chain structure terminated by a hydrogen atom on each end.[22–24] As these isolated boron clusters have planar geometries and exhibit aromatic and antiaromatic electronic properties analogous to hydrocarbons, they can potentially be building blocks of new solids and large boron cages.[8] Therefore, we attempt to design a possible bottom-up synthesis of the boron cages and fullerenes from these small planar clusters.

Different with the carbon cages and graphene, the double chain structure plays an important role in the medium boron clusters and two-dimensional (2D) boron sheets. The planar-to-tubular structural transition starts at B_{20} for neutral clusters[17,25] and the stable B_{20}, B_{22}, B_{24}, B_{32}, and B_{36} clusters are closed double chains (double rings).[17,26–30] The double-chain hexagonal $B_{18}H_4$ cluster is a perfectly planar concentric π-aromatic borannulene, which is the smallest boron hydride cluster with a hexagonal hole.[31] The stable two-dimensional boron sheets, such as α-, β-, $\eta_{2/15}$-, and $\eta_{4/28}$-sheets are completely or partially interweaved by the double chains.[32–40] In particular, the unusual stability of B_{80} fullerene can be explained by its structure of six interwoven double-ring clusters.[1]

From the top-down view of point, the B_{80} fullerene (Fig. 1(a)) can be decomposed into three B_{12} fragments and a spherical B_{44} skeleton (Fig. 1(b)), which can be further decomposed into two hexagonal B_7 and three double-chain B_{10} clusters (Fig. 1(c)). The B_{44} skeleton will be called three-chain cages for short because it is spherical and consists mainly of three boron double-chains. As mentioned above, the hexagonal B_7 and a series of double-chain clusters, B_2, B_4, B_6, B_8H_2, $B_{10}H_2$, $B_{12}H_2$, and the double-ring B_{20}, had been produced by the laser vaporization of a boron target.[8,22] Therefore, a series of three-chain boron cage could be synthesized from these small planar clusters, and these three-chain cages should be used to further synthesize the boron fullerenes.

In this work, we will investigate the geometric structures, the stability, and the possible synthesis pathway of a series of three-chain B_{6n+14} (n = 1–12) cages using the density functional theory (DFT). Beside the B_{80} fullerene, we also predicted formation of B_{44} and B_{59} fullerenes by patching the three-chain B_{32} and B_{38} cages with the B_4 and B_7 clusters, respectively.

Since it had been proven that only the PBE,[41] PBE0,[42] TPSS,[43] and TPSSh[44,45] functionals give the same energy order of the B_{20} isomers as the CCSD(T) predicts,[5] the geometry optimizations were performed at the PBE0/6-31G(d,p) and TPSSh/6-31G(d,p) levels, respectively. The optimized geometric structures of three-chain boron cages have only some negligible difference using the different functionals so that

[a]Email: luhg@sxu.edu.cn

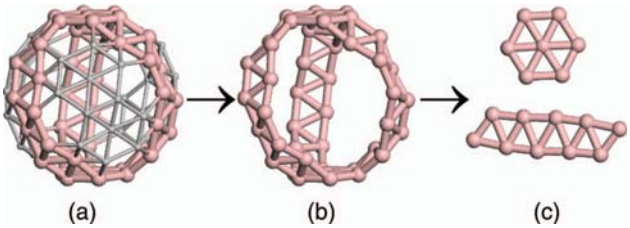

FIG. 1. The top-down decompositions of fullerene B_{80} into small boron clusters: (a) B_{80} fullerene, (b) three-chain B_{44} cage, and (c) the hexagonal B_7 and the double-chain B_{10} clusters.

only the PBE0 functional was used in the following investigations. For each cage, vibrational frequencies were calculated at the PBE0/6-31G(d,p) level to ensure that the cage corresponded to the minimum on the potential energy surface. The single-point electronic energies were calculated at the PBE0/6-311+G(2d,p)//PBE0/6-31G(d,p) level. All PBE0 and TPSSh calculations of clusters were carried out using the Gaussian 09 program.[46] The PBE calculations of clusters and 2D sheets were performed with the VASP 5.2 package[47,48] using the projector augmented wave (PAW) method[49] and a planewave basis set with a 500 eV kinetic energy cutoff. The Brilliouin zone is sampled using k-points with 0.02 $Å^{-1}$ spacing in the Monkhorst–Pack scheme.[50] The boron clusters are placed in a cubic box with a length of 30 Å, and the 2D boron sheets are represented by unit cell with a 30 Å vacuum region in the normal direction. For geometric optimization, both lattice constants and positions of atoms are fully relaxed. Upon optimization, the forces on all atoms are less than 0.01 eV/Å and the criterion for total energy convergence is 0.1 meV/atom.

The shapes and properties of the three-chain B_{6n+14} (n = 1–12) cages are depicted in Fig. 2 and Table I. The shapes of B_{6n+14} (n = 2–12) are approximately spherical, and their average radii range from 2.54 to 7.57 Å, with maximum relative deviations no more than 13%. In contrast to the boron fullerenes which have only pentagonal and/or hexagonal holes, these three-chain cages have three large holes. In addition, the three-chain B_{20} cage in Figs. 2(a) and 2(b) is an oblate spheroid with three hexagonal holes, and is 0.103 eV/atom less stable than its famous double-ring B_{20} isomer. Therefore, the three-chain B_{20} cage is one of the possible low-lying fullerene isomers of the double-ring B_{20}.[5]

Since the three-chain B_{6n+14} (n = 1–12) cages can be decomposed into three B_{4+2n} semi-double-rings, it is interesting to compare the stability between the three-chain cages and their double-ring isomers. In Fig. 3, we have plotted the cohesive energies (E_c) of the three-chain cages and the double-rings B_{6n+14} (n = 1–12). From B_{20} to B_{86} (Fig. 2), the cohesive energies of the three-chain cages increase from 5.24 eV to 5.54 eV, while those of double-rings from 5.37 eV to 5.54 eV. Though the small three-chain cages B_{6n+14} (n = 1–4) are obviously less stable than their double-ring isomers, the large ones, B_{6n+14} (n = 5–12), are nearly as stable as their double-ring isomers.

In addition, the stability of the large three-chain cages, B_{6n+14} (n = 6–12), shows a slight odd-even fluctuation. As shown in Fig. 3, the three-chain B_{6n+14} (n = 7, 9, and 11) cages are slightly less stable than their neighbors. This odd-even fluctuation is in agreement with the odd-even alternations of highest occupied molecular orbital-lowest unoccupied molecular orbital (HOMO-LUMO) energy separation (Table I), which serves as a simple measure of chemical stability.[1]

In order to further verify the stability of these three-chain cages, we performed the first principle molecular dynamics (FPMD) simulations using the QUICKSTEP module of CP2K2.3 suite[51,52] at the temperatures of 200, 500, and 700 K for 3.0 ps, respectively. The temperatures at which their geometric structures are maintained are 200 K for B_{20}, 500 K for B_{26}, and 700 K for the B_{6n+14} (n = 3–12) cages, respectively (see supplementary material[53]). Consequently, most of the three-chain cages in Fig. 2 are stable in high temperature, except B_{20} and B_{26}. To assist future experiments, we presented the computed vertical electron affinity (E_{VEA}) values and HOMO-LUMO ($E_{H\text{-}L}$) gaps of these three-chain B_{6n+14} (n = 1–12) cages in Table I.

Though the optimized structures of the three-chain B_{6n+14} cages have different symmetries (D_3, C_3, C_2, and C_1, Table I), they have approximate symmetry of C_3 for odd n and of D_3 for even n. Therefore, the structures of these three-chain boron cages in Fig. 2 are very simple to facilitate their bottom-up syntheses from the hexagonal B_7 cluster and the double-chain boron or boron-rich clusters (B_2, B_4, B_6, B_8H_2,

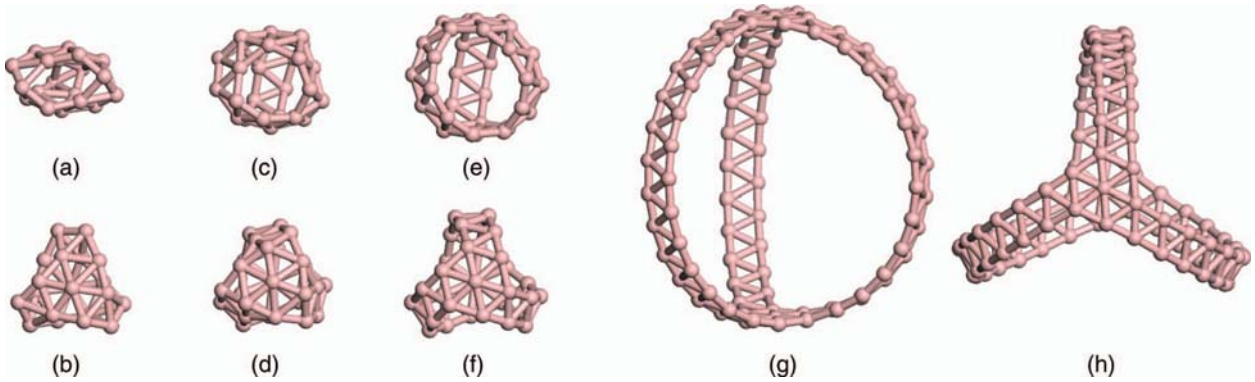

FIG. 2. The side and top views of some three-chain cages: B_{20} ((a) and (b)), B_{26} ((c) and (d)), B_{32} ((e) and (f)), and B_{86} ((g) and (h)).

TABLE I. The geometric and energetic properties of the three-chain B_{6n+14} (n = 1–12) cages and the $B_{44}{}^{f}$, $B_{59}{}^{f}$, and $B_{80}{}^{f}$ fullerenes.[a]

Cage	Sym.	r_{avg}	Δr_{max}	$\Delta r/r_{avg}$	E_c	$E_{H\text{-}L}$	E_{VEA}	ΔH	E_c'	E_{2D}	ΔE_c
B_{20}	C_2	2.17	0.70	32.4	5.24	2.23	2.29	−3095.7	5.37	5.81	0.44
B_{26}	C_3	2.54	0.33	12.9	5.35	2.42	2.17	−2893.2	5.53	5.76	0.23
B_{32}	C_3	3.08	0.30	9.6	5.41	1.88	3.01	−3179.5	5.55	5.74	0.19
B_{38}	D_3	3.55	0.42	11.8	5.45	1.88	2.84	−1743.6	5.58	5.73	0.15
B_{44}	C_2	4.06	0.22	5.3	5.48	1.39	3.62	−2016.1	5.58	5.72	0.14
B_{50}	C_3	4.54	0.34	7.5	5.50	1.69	3.18	−1865.9	5.63	5.72	0.09
B_{56}	C_2	5.05	0.25	5.0	5.51	1.06	3.99	···	5.63	5.72	0.09
B_{62}	C_3	5.55	0.26	4.6	5.52	1.39	3.38	···	5.65	5.71	0.06
B_{68}	C_1	6.06	0.31	5.1	5.52	0.76	4.23	···	5.65	5.71	0.06
B_{74}	C_3	6.56	0.19	2.9	5.54	1.17	3.87	−2257.5	5.66	5.71	0.05
B_{80}	C_1	7.06	0.31	4.3	5.53	0.57	4.38	−2291.1	5.66	5.71	0.05
B_{86}	C_3	7.57	0.16	2.0	5.54	1.03	4.11	−2164.1	5.67	5.71	0.04
$B_{44}{}^{f}$	C_1	3.16	1.11	35.0	5.43	1.63	3.13	−2016.4			
$B_{59}{}^{f}$	C_1	3.57	0.76	21.3	5.52	1.42	3.11	−2148.0			
$B_{80}{}^{f}$	T_h	4.12	0.40	9.6	5.64	2.12	2.94	−6510.0			

[a]The Sym., r_{avg}, Δr_{max}, and $\Delta r/r_{avg}$ are the symmetry, average radii (Å), maximum deviations of radius (Å), and maximum relative deviations of radius (%), respectively. The E_c, $E_{H\text{-}L}$, E_{VEA}, and E_c' are the cohesive energies (eV/atom) including zero-point energy correction, HOMO-LUMO energy separations (eV), vertical electron affinity (eV) at the PBE0 level, and the cohesive energies (eV/atom) using VASP 5.2 package at the PBE level, respectively. E_{2D} is the cohesive energy (eV/atom) of the corresponding 2D boron sheets. ΔE_c is the difference of cohesive energies between the 2D boron sheet and its corresponding cluster. ΔH is the standard formation enthalpy (kJ/mol) of the three-chain B_{6n+14} (n = 1–12) cages (from the B_7 and $B_{2n}/B_{2n}H_2$ clusters) and the $B_{44}{}^{f}$, $B_{59}{}^{f}$, and $B_{80}{}^{f}$ fullerenes (from the corresponding three-chain precursors and the small planar fragments).

$B_{10}H_2$, $B_{12}H_2$, B_{20}, B_{22}, and B_{24}). However, the synthesis pathways for the three-chain B_{56}, B_{62}, and B_{68} cages are still unpredictable because of the absence of the double-chain B_{14}, B_{16}, and B_{18} clusters in experiment as well as theoretical prediction.

From the experimentally synthesized and theoretically predicted double-chain clusters, the three-chain cages may be bottom-up synthesized by three types of reactions: (a) $2B_7 + 3B_{2n} = B_{6n+14}$ (n = 1–3), (b) $2B_7 + 3B_{2n}H_2 = B_{6n+14} + 3H_2$ (n = 4–6), and (c) $2B_7 + 3B_{2n} = B_{6n+14}$ (n = 10–12) (Figs. 4(a)–4(c), respectively). Though these reactions are strongly exothermic and their standard enthalpies are from −1743.6 to −3095.7 kJ/mol (Table I), the production of the three-chain B_{6n+14} cages remains a challenge because their two reactants can yield many other possible products, such as the 2D boron sheets and 1D nanotubes.

The 2D B_{6n+14} parallelogram sheets (Fig. 5(a)) that are formed by the hexagonal B_7 and double-chain $B_{2n}/B_{2n}H_2$

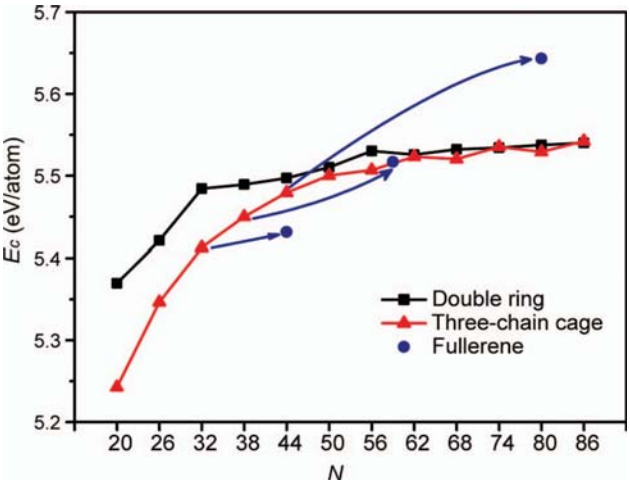

FIG. 3. Cohesive energy (E_c) per atom as a function of the number of atoms (N) in the B_N clusters. The squares, the triangles, and the circles correspond to the double rings, the three-chain cages, and the boron fullerenes patched from the three-chain cages. The arrows show increases in cohesive energy after being patched with the small clusters.

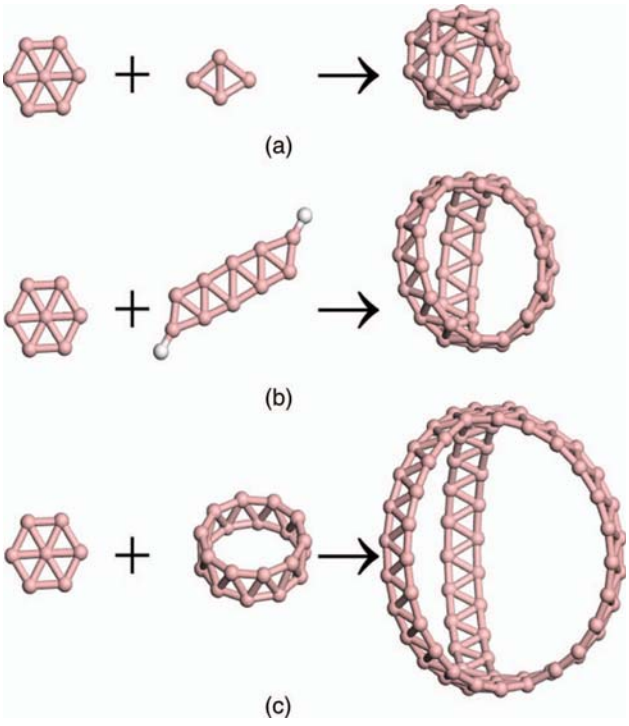

FIG. 4. The bottom-up syntheses of the three-chain B_{26} (a), B_{44} (b), and B_{74} (c) cages from B_7 and B_4, $B_{10}H_2$, and B_{20} clusters, respectively.

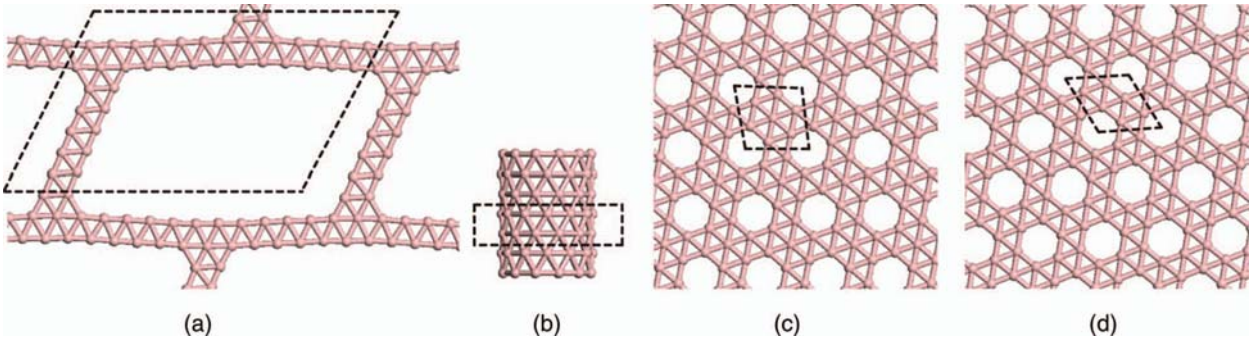

FIG. 5. ((a)–(d)) The geometric structures of the 2D B_{38} sheet (a representative B_{6n+14} sheet), 1D B_{24} tube, α_1- and snub-sheets.

are more stable than their corresponding clusters in thermodynamics (Table I). Except B_{20}, the differences (ΔE_c) of cohesive energies between the 2D B_{6n+14} (n = 2–12) sheets and their corresponding three-chain clusters are only 0.04–0.23 eV/atom (Table I) and much less than that (0.38 eV/atom at the PBE level using VASP 5.2 package) between the graphene and C_{60} fullerene. The three-chain B_{6n+14} (n = 1–12) cages may also be formed by the graphene-to-fullerene-like transformation[54] from their 2D parallelogram isomers. Consequently, both the three-chain B_{6n+14} (n = 2–12) cages and their 2D parallelogram isomers should be yielded in experiment.

Because of the highly reactive nature of the B_n clusters, the reactant species can individually form 1D tubes or 2D sheets. The double-ring B_{20}, B_{22}, and B_{24} can form the 1D tubes (Fig. 5(b)) with cohesive energies of 5.49, 5.51, and 5.52 eV/atom, respectively, which indicates that the 1D B_{20}, B_{22}, and B_{24} tubes are less stable than their three-chain products (B_{6n+14} cages, n = 10–12). The hexagonal B_7 and the double-chain B_6 can form the α_1- and snub-sheets with the cohesive energies of 5.95 and 5.93 eV/atom, respectively (Figs. 5(c) and 5(d)).[34,55] Obviously, the α_1- and snub-sheets are more stable than the three-chain boron clusters as well as their 2D parallelogram isomers. To avoid the formation of the α_1- and snub-sheets, we can choose the charged B_7 and $B_{2n}/B_{2n}H_2$ reactants. Therefore, the (charged) three-chain boron cages and the 2D parallelogram sheets should be yielded selectively from $B_7^+ + B_{2n}^-/B_{2n}H_2^-$ or $B_7^- + B_{2n}^+/B_{2n}H_2^+$ reactants, whose cluster beam should be produced by laser vaporization of a boron target with helium (containing some H_2 as needed) as the carrier gas and should be mass-selected using time-of-flight mass spectrometry.[22]

The spherical structure with three large holes and a cavity of the three-chain cages B_{6n+14} (n = 3–12) in Fig. 2 implies that they could be taken as the possible precursors for the bottom-up syntheses of the boron fullerenes as well as the "core-shell" stuffed boron fullerenes. Our calculations demonstrated that the three-chain cages B_{32} and B_{38} could be patched with three rhombic B_4 and three hexagonal B_7 clusters to yield the B_{44}^f and B_{59}^f fullerenes, respectively (Figs. 6(a) and 6(b)). Similarly, the three-chain B_{44} cage can form the B_{80}^f fullerene by patching concomitantly with three B_7 and three B_5 planar clusters (Fig. 6(c)). These reactions are also strongly exothermic in thermodynamics and their standard enthalpies of reaction are −2016.4, −2148.0, and −6510.0 kJ/mol for the B_{44}, B_{59}, and B_{80} fullerenes, respectively (Table I). The cohesive energies of the B_{44}, B_{59}, and B_{80} fullerenes increase by about 0.02, 0.07, and 0.16 eV/atom more than those of the three-chain B_{32}, B_{38}, and B_{44} cages, respectively (Table I and Fig. 3). In particular, the three-chain skeletons are almost preserved in the patched fullerenes, which means that the three-chain B_{6n+14} cages should play an essential role in the bottom-up syntheses of the boron fullerenes. Furthermore, when some small boron clusters or metal atom(s) can be stuffed in the core of the three-chain boron cages, the "core-shell"-type boron fullerenes or the endohedral metalloborofullerenes[56,57] should be formed.

In summary, a series of three-chain boron cages B_{6n+14} (n = 1–12) were proposed with the structure of three fused

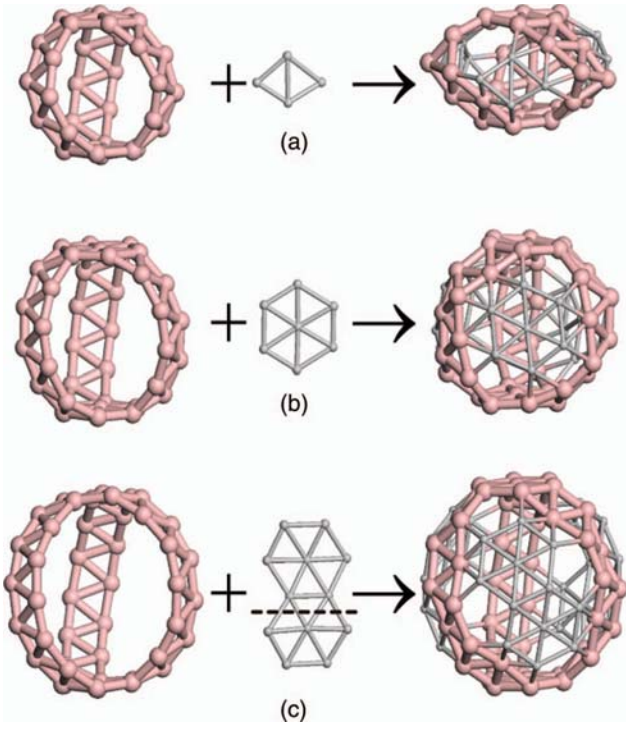

FIG. 6. The bottom-up syntheses of boron fullerenes from the three-chain B_{32}, B_{38}, and B_{44} cages to the B_{44}^f (a), B_{59}^f (b), and B_{80}^f (c) fullerenes, respectively.

semi-double-rings. Though some of them are less stable than their double ring isomers, their simple geometric structures facilitate the bottom-up syntheses from the small planar boron clusters. Their formation reactions from the hexagonal B_7 and the double-chain boron clusters are strongly competed by their 2D parallelogram sheets and the other 2D sheets. To avoid the formation of the α_1- and snub-sheets of the individual B_n reactant species, the optimal reactants should be $B_7^+ + B_{2n}^-/B_{2n}H_2^-$ or $B_7^- + B_{2n}^+/B_{2n}H_2^+$ to yield selectively the three-chain boron cages in gas. Because of their spherical shapes, the three-chain B_{6n+14} cages can be taken as the possible precursors to synthesize the boron fullerenes, such as B_{44}, B_{59}, and B_{80} fullerenes. Consequently, the three-chain boron cages provide a possible synthesis pathway of the boron fullerenes and metalloborofullerenes towards their experimental realizations and applications in material science.

The authors thank the anonymous reviewers for their valuable comments.

[1]N. G. Szwacki, A. Sadrzadeh, and B. Yakobson, Phys. Rev. Lett. **98**, 166804 (2007).
[2]H. Li, N. Shao, B. Shang, L. Yuan, J. Yang, and X. C. Zeng, Chem. Commun. (Cambridge) **46**, 3878 (2010).
[3]J. Zhao, L. Wang, F. Li, and Z. Chen, J. Phys. Chem. A **114**, 9969 (2010).
[4]D. Jiang, M. Walter, and S. Dai, Chem.-Eur. J. **16**, 4999 (2010).
[5]F. Li, P. Jin, D. Jiang, L. Wang, S. B. Zhang, J. Zhao, and Z. Chen, J. Chem. Phys. **136**, 074302 (2012).
[6]S. De, A. Willand, M. Amsler, P. Pochet, L. Genovese, and S. Goedecker, Phys. Rev. Lett. **106**, 225502 (2011).
[7]P. Boulanger, M. Morinière, L. Genovese, and P. Pochet, J. Chem. Phys. **138**, 184302 (2013).
[8]A. N. Alexandrova, A. I. Boldyrev, H. J. Zhai, and L. S. Wang, Coord. Chem. Rev. **250**, 2811 (2006).
[9]D. Y. Zubarev and A. I. Boldyrev, J. Comput. Chem. **28**, 251 (2007).
[10]Z. H. Zhai, L. S. Wang, A. N. Alexandrova, A. I. Boldyrev, and V. G. Zakrzewski, J. Phys. Chem. A **107**, 9319 (2003).
[11]A. N. Alexandrova, A. I. Boldyrev, H. J. Zhai, L. S. Wang, E. Steiner, and P. W. Fowler, J. Phys. Chem. A **107**, 1359 (2003).
[12]H. J. Zhai, B. Kiran, J. Li, and L. S. Wang, Nature Mater. **2**, 827 (2003).
[13]H. J. Zhai, A. N. Alexandrova, K. A. Birch, A. I. Boldyrev, and L. S. Wang, Angew. Chem., Int. Ed. **42**, 6004 (2003).
[14]A. N. Alexandrova, A. I. Boldyrev, H. J. Zhai, and L. S. Wang, J. Phys. Chem. A **108**, 3509 (2004).
[15]A. N. Alexandrova, H. J. Zhai, L. S. Wang, and A. I. Boldyrev, Inorg. Chem. **43**, 3552 (2004).
[16]A. N. Alexandrova, A. I. Boldyrev, H. J. Zhai, and L. S. Wang, J. Chem. Phys. **122**, 054313 (2005).
[17]B. Kiran, S. Bulusu, H. J. Zhai, S. Yoo, X. C. Zeng, and L. S. Wang, Proc. Natl. Acad. Sci. U.S.A. **102**, 961 (2005).
[18]A. P. Sergeeva, D. Y. Zubarev, H. J. Zhai, A. I. Boldyrev, and L. S. Wang, J. Am. Chem. Soc. **130**, 7244 (2008).
[19]W. Huang, A. P. Sergeeva, H. J. Zhai, B. B. Averkiev, L. S. Wang, and A. I. Boldyrev, Nat. Chem. **2**, 202 (2010).
[20]I. Boustani, Phys. Rev. B **55**, 16426 (1997).
[21]I. Boustani, Chem. Modell. **8**, 1 (2011).
[22]W. L. Li, C. Romanescu, T. Jian, and L. S. Wang, J. Am. Chem. Soc. **134**, 13228 (2012).
[23]D.-Z. Li, Q. Chen, Y.-B. Wu, H.-G. Lu, and S.-D. Li, Phys. Chem. Chem. Phys. **14**, 14769 (2012).
[24]H. Bai, Q. Chen, C.-Q. Miao, Y.-W. Mu, Y.-B. Wu, H.-G. Lu, H.-J. Zhai, and S.-D. Li, Phys. Chem. Chem. Phys. **15**, 18872 (2013).
[25]W. An, S. Bulusu, Y. Gao, and X. C. Zeng, J. Chem. Phys. **124**, 154310 (2006).
[26]A. P. Sergeeva, Z. A. Piazza, C. Romanescu, W.-L. Li, A. I. Boldyrev, and L.-S. Wang, J. Am. Chem. Soc. **134**, 18065 (2012).
[27]M. A. L. Marques and S. Botti, J. Chem. Phys. **123**, 014310 (2005).
[28]I. Boustani and A. Quandt, Europhys. Lett. **39**, 527 (1997).
[29]I. Boustani, A. Rubio, and J. Alonso, Chem. Phys. Lett. **311**, 21 (1999).
[30]S. Chacko, D. G. Kanhere, and I. Boustani, Phys. Rev. B **68**, 035414 (2003).
[31]Q. Chen, H. Bai, J.-C. Guo, C.-Q. Miao, and S.-D. Li, Phys. Chem. Chem. Phys. **13**, 20620 (2011).
[32]H. Tang and S. Ismail-Beigi, Phys. Rev. Lett. **99**, 115501 (2007).
[33]E. S. Penev, S. Bhowmick, A. Sadrzadeh, and A. I. Yakobson, Nano Lett. **12**, 2441 (2012).
[34]X. J. Wu, J. Dai, Y. Zhao, Z. W. Zhuo, J. L. Yang, and X. C. Zeng, ACS Nano **6**, 7443 (2012).
[35]H. Lu, Y. Mu, and S.-D. Li, ACS Nano **7**, 879 (2013).
[36]X. J. Wu, J. Dai, Y. Zhao, Z. W. Zhuo, J. L. Yang, and X. C. Zeng, ACS Nano **7**, 880 (2013).
[37]X. Yu, L. Li, X. Xu, and C. Tang, J. Phys. Chem. C **116**, 20075 (2012).
[38]H. Lu, Y. Mu, H. Bai, Q. Chen, and S.-D. Li, J. Chem. Phys. **138**, 024701 (2013).
[39]D. Yu. Zubarev and A. I. Boldyrev, Phys. Chem. Chem. Phys. **10**, 5207 (2008).
[40]T. R. Galeev, Q. Chen, J.-C. Guo, H. Bai, C.-Q. Miao, H.-G. Lu, A. P. Sergeeva, S.-D. Li, and A. I. Boldyrev, Phys. Chem. Chem. Phys. **13**, 11575 (2011).
[41]J. P. Perdew, K. Burke, and M. Ernzerhof, Phys. Rev. Lett. **77**, 3865 (1996).
[42]C. Adamo and V. Barone, J. Chem. Phys. **110**, 6158 (1999).
[43]J. Tao, J. P. Perdew, V. N. Staroverov, and G. E. Scuseria, Phys. Rev. Lett. **91**, 146401 (2003).
[44]J. P. Perdew, S. Kurth, A. Zupan, and P. Blaha, Phys. Rev. Lett. **82**, 2544 (1999).
[45]J. P. Perdew, J. Tao, V. N. Staroverov, and G. E. Scuseria, J. Chem. Phys. **120**, 6898 (2004).
[46]M. J. Frisch, G. W. Trucks, H. B. Schlegel *et al.*, GAUSSIAN 09, Revision A.01, Gaussian, Inc., Wallingford, CT, 2009.
[47]G. Kresse and J. Furthmüller, Comput. Mater. Sci. **6**, 15 (1996).
[48]G. Kresse and J. Furthmüller, Phys. Rev. B **54**, 11169 (1996).
[49]P. E. Blöchl, Phys. Rev. B **50**, 17953 (1994).
[50]H. J. Monkhorst and J. D. Pack, Phys. Rev. B **13**, 5188 (1976).
[51]See http://cp2k.berlios.de/ for the CP2K developers group, 2000–2012.
[52]J. VandeVondele, M. Krack, F. Mohamed, M. Parrinello, T. Chassaing, and J. Hutter, Comput. Phys. Commun. **167**, 103 (2005).
[53]See supplementary material at http://dx.doi.org/10.1063/1.4839575 for the first principle molecular dynamics simulations of B_{20} at 200 K, B_{26} at 500 K, and B_{32}, B_{38}, B_{44}, and B_{86} at 700 K.
[54]A. Chuvilin, U. Kaiser, E. Bichoutskaia, N. A. Besley, and A. N. Khlobystov, Nat. Chem. **2**, 450 (2010).
[55]R. R. Zope and T. Baruah, Chem. Phys. Lett. **501**, 193 (2011).
[56]J.-T. Wang, C. Chen, E. G. Wang, D.-S. Wang, H. Mizuseki, and Y. Kawazoe, Appl. Phys. Lett. **94**, 133102 (2009).
[57]P. Jin, C. Hao, Z. Gao, S. B. Zhang, and Z. Chen, J. Phys. Chem. A **113**, 11613 (2009).